Molecular Diversity
https://doi.org/10.1007/s11030-020-10156-5

ORIGINAL ARTICLE

Synthesis and biological evaluation in vitro and in silico of *N*-propionyl-*N′*-benzeneacylhydrazone derivatives as cruzain inhibitors of *Trypanosoma cruzi*

Timoteo Delgado-Maldonado[1] · Benjamín Nogueda-Torres[2] · José C. Espinoza-Hicks[3] · Lenci K. Vázquez-Jiménez[1] · Alma D. Paz-González[1] · Alfredo Juárez-Saldívar[1] · Gildardo Rivera[1]

Received: 3 June 2020 / Accepted: 4 November 2020

Abstract

An *N*-acylhydrazone scaffold has been used to develop new drugs with diverse biological activities, including trypanocidal activity against different strains of *Trypanosoma cruzi*. However, their mechanism of action is not clear, although in *T. cruzi* it has been suggested that the enzyme cruzain is involved. The aim in this work was to obtain new *N*-propionyl-*N′*-benzeneacylhydrazone derivatives as potential anti-*T. cruzi* agents and elucidate their potential mechanism of action by a molecular docking analysis and effects on the expression of the cruzain gene. Compounds **9** and **12** were the most active agents against epimastigotes and compound **5** showed better activity than benznidazole in *T. cruzi* blood trypomastigotes. Additionally, compounds **9** and **12** significantly increase the expression of the cruzain gene. In summary, the in silico and in vitro data presented herein suggest that compound **9** is a cruzain inhibitor.

Graphic abstract

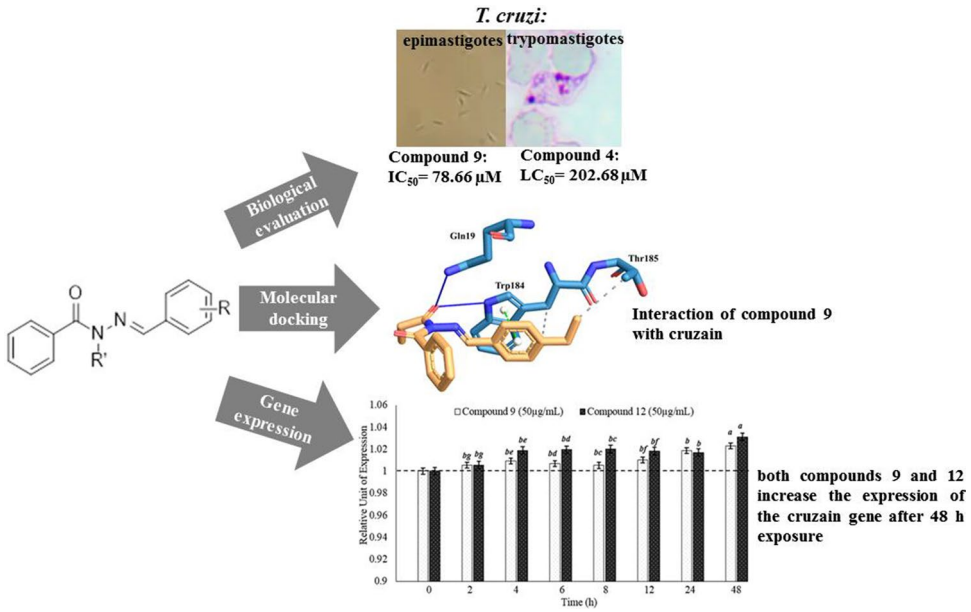

Electronic supplementary material The online version of this article (https://doi.org/10.1007/s11030-020-10156-5) contains supplementary material, which is available to authorized users.

Extended author information available on the last page of the article

Published online: 20 November 2020

Keywords *N*-propionyl-*N*′-benzeneacylhydrazone · Molecular docking · Cruzain · *Trypanosoma cruzi*

Introduction

The protozoan parasite *Trypanosoma cruzi* (*T. cruzi*) is the causal agent of American trypanosomiasis, also called Chagas disease, which is technically transmitted enzootically [1, 2]. Chagas disease is endemic in 21 Latin American countries, but recently different cases have been reported in Canada, Australia, Japan and Europe, suggesting that it has become a global health problem [3–5].

According to the World Health Organization (WHO) and the Center for Disease Control and Prevention (CDC), Chagas disease affects 8 to 10 million people worldwide [6], with an annual mortality of 10,000 people, which translates into economic losses that exceed millions of dollars in control and prevention efforts [7].

The only drugs available are nifurtimox (Nfx) and benznidazole (Bzn). However, Nfx and Bzn are not adequate drugs because they cause severe adverse effects and have poor efficacy in the chronic phase. Also, there are strains resistant to these drugs, which are not over-the-counter [8, 9]. Therefore, there is a need to develop new molecules with biological activity against *T. cruzi*. In that sense, small molecules (molecular weight < 500) of easy synthesis have been reported as new trypanocidal agents [10, 11].

In the last two decades, one of the most relevant strategies is the development of inhibitors of pharmacological targets exclusive of the parasite; such is the case of the cruzain enzyme, which is a cysteine-protease abundant in *T. cruzi*, and essential for its metabolism. Currently, cruzain continues to be one of the most relevant targets for the design of new anti-Chagas drugs, since it has been validated through biochemical studies and in vivo models [12–14].

In medicinal chemistry, the chemical moiety of *N*-acylhydrazone (NAH, Fig. 1) is recognized as a privileged structure because it has diverse biological activities toward different therapeutic targets [15–17]. In previous studies, *N*-acylhydrazone derivatives have been used as new approaches in developing drugs to combat Chagas disease; for example, Romeiro et al. [18] designed and synthesized quinoxaline-*N*-acylhydrazone derivatives using classical bioisosterism; **LASSBio-1016** (Fig. 1A) had trypanocidal activity (IC_{50} = 15.9 µM) against epimastigotes of the Tulahuen 2 strain of *T. cruzi*. In another study carried out by Massarico et al. [19], hybrid derivatives of *N*-acylhydrazone and furoxanes were evaluated as new trypanocidal agents; compound **6** (Fig. 1B) showed trypanocidal activity in vitro against amastigotes (Tulahuen C2C4 strain). Also, this compound was shown to be a cruzain inhibitor with IC_{50} values of 11.2 ± 0.2 µM.

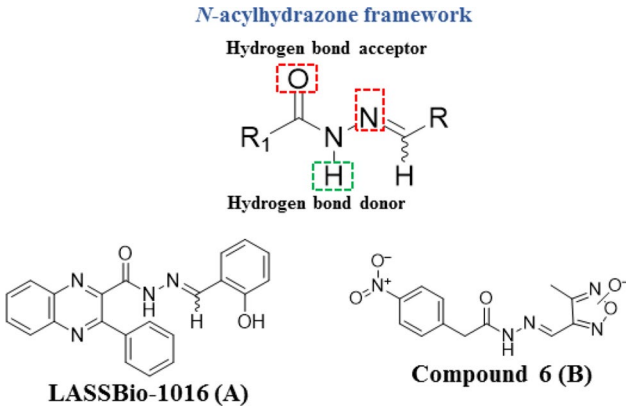

Fig. 1 Structure of NAH derivatives tested as trypanocidal agents

In 2017, Elizondo-Jiménez et al. [20] reported the synthesis and biological evaluation of new benzenesulfonylhydrazones. Interestingly, compound **4** (Fig. 2) was active against both NINOA and INC-5 strains of *T. cruzi* (LC_{50} = 26.3 and 4.68 µM, respectively), and compound **11** (Fig. 2) that incorporates an *N*-acyl group presented LC_{50} values below 2 µM against trypomastigotes of the INC-5 strain. Therefore, the importance of sulfonyl and/or acyl groups is not clear. Also, the authors suggest that these compounds could be binding with cruzain by molecular docking. Based on the above, in this work, it was decided to change the sulfonyl group (–SO_2) by an acyl group (–CO–) to obtain new *N*-propionyl-*N*′-benzeneacylhydrazone derivatives and evaluate their trypanocidal activity. Additionally, their mode of binding on the active site of cruzain and their effect on the expression of the cruzain gene in epimastigotes of *T. cruzi* were evaluated to elucidate its possible mechanism of action.

Materials and methods

Chemistry

All reagents were purchased from Sigma Aldrich Chemical Co. and used without further purification. Reaction progress was monitored using thin-layer chromatography (TLC) aluminum oxide matrix Z234214-1PAK sheets from Sigma Aldrich®. Column chromatography was performed using silica gel 60A (230–400 mesh) and solvents employed were of analytical grade. Infrared (IR) spectra were recorded on an FT-IR Bruker Tensor 27 spectrophotometer coupled to Bruker platinum ATR cell. Mass spectrometry ESI–MS analyses were conducted on an Ultra Performance Liquid Cromatography-Mass Spectrometer (UPLC-MS) waters. Nuclear magnetic resonance (NMR) spectra (^1H and ^{13}C) were measured on a Bruker Ultrashield-400 spectrometer, using DMSO-d_6 as a solvent and some cases TMS

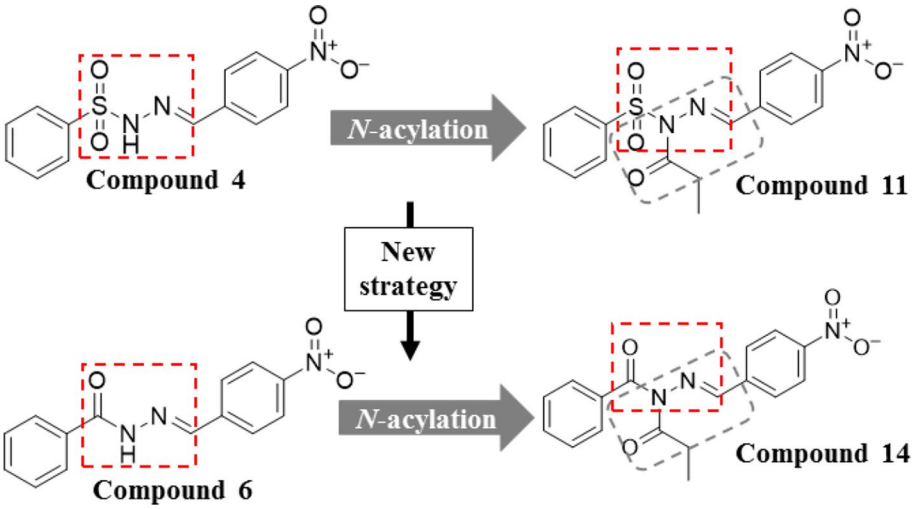

Fig. 2 Structural modification to obtain new benzene-sulfonyl-hydrazide analog derivatives

as reference. Chemical shifts are presented on the δ scale (ppm). Multiplicities are indicated as follows: s (singlet), d (doublet), t (triplet), m (multiplet) or br (broad).

The general procedure for the preparation of *N′*-[(*E*)-phenylmethylidene]benzeneacylhydrazone derivatives (BAH series) was as follows: in a 50-mL round-bottomed flask 30 mL of ethanol, benzhydrazide (1 mmol) and aldehyde derivative (1 mmol) were added at room temperature and in constant agitation, HCl drops (37%) were used as a catalyst. After, the mixture was refluxed for 3–6 h and the progress of the reaction was monitored by TLC. Finally, the reaction product was purified by column chromatography using *n*-hexane: ethyl acetate (98:2).

The synthesis of *N*-propionyl-*N′*-[(*E*)-phenylmethylidene] benzeneacylhydrazone derivatives (BAH-N series), 30 mL of dry dichloromethane, the previously obtained benzeneacylhydrazone derivative (1 mmol) and dry triethylamine (3 mmol) were added drop by drop at 0 °C and the mixture was stirred for 1 h. After, propionyl chloride (1.5 mmol) was added dropwise and stirring was continued for additional 24–48 h at room temperature. The reaction mixture was purified by column chromatography using *n*-hexane: ethyl acetate (98:2) and crystallized into dichloromethane/*n*-hexane.

Biological activity

Epimastigotes

The NINOA strain of epimastigotes *T. cruzi* was cultured and preserved in Brain Heart Infusion (BHI) medium supplemented with 10% Fetal Bovine Serum (FBS) and 1% penicillin/streptomycin at 500 µg/mL incubated at 28 °C. To keep the strain viable, transfers were made every 5–7 days to a fresh medium. At all times, work was carried out under sterile conditions.

The trypanocidal evaluation of BAH and BAH-N series was performed against epimastigotes of *T. cruzi* in triplicate assays. BHI medium supplemented with 10% FBS and 1% penicillin/streptomycin (500 µg/mL) was prepared for this purpose. After, 90 µL of epimastigotes 1×10^6 cells/mL and 10 µL of each compound at 50 µg/mL dissolved in dimethylsulfoxide (DMSO) at 1% were added to a 96-well plate. Negative control of untreated epimastigotes and the reference drugs Nfx and Bzn were included as positive controls. The plate was incubated at 28 °C for 24 h, then 10 µL of 3-(4,5-dimethylthiazol-2-yl)-2,5-diphenyl tetrazolium bromide (MTT) at 2.5 mg/mL in 1X phosphate-buffered saline (PBS) was added and incubated for 4 h at 37 °C. Subsequently, 100 µL of sodium dodecyl sulfate-hydrochloric acid (SDS-HCl; 10%-0.01 N) were added to dissolve the MTT crystals and again incubated at 28 °C for 24 h. The optical density (OD) was determined at 595 nm and all absorbances were corrected for a blank (medium BHI + FBS + Antibiotic) by subtracting its absorbance value from each of the samples (OD_{595} blank—OD_{595} sample). The mortality percentage was calculated using the following formula: $100 - (OD(t)/OD(c) \times 100)$, where OD(*t*) is the optical density of the culture after exposure to the compound evaluated and OD(c) is the optical density of the untreated control culture. The half maximal inhibitory concentration (IC_{50}) was determined from five concentrations serial two-fold (50 µg/mL to 3.12 µg/mL) for each compound using the Probit statistical tool. Later the results were converted to micromolar units.

Trypomastigotes

Blood trypomastigotes of NINOA strain of *T. cruzi* were obtained from CD1 mice by cardiac puncture after 15 days post-infection when parasitemia was highest. To keep the

trypomastigotes viable, transfers were made to CD1 mice of 20 days of age with a weight of 24–26 g. At all times we worked under sterile conditions and in accordance with Law NOM-062-ZOO-1999 [21]. Animals were sacrificed in accordance with international guidelines on the care and use of animals in research.

BAH and BAH-N series, as well as Nfx and Bzn controls, were evaluated in triplicate. After, 90 µL of blood containing blood trypomastigotes (4.5×10^5 cells/mL) and 10 µL of each derivative to 50 µg/mL dissolved in 1% DMSO were added to a 96-well plate. An untreated negative control was included. The plate was incubated at 4 °C for 24 h, and then the trypomastigotes were quantified according to Brener's method [22]. The trypanocidal activity was expressed as a percentage of lysis with respect to untreated control. The half maximal lytic concentration (LC_{50}) was determined from five concentrations (100, 50, 40, 20 and, 10 µg/mL) for each compound using the Probit statistical tool. Later the results were converted to micromolar units.

Molecular docking

The molecular binding analysis of BAH and BAH-N series on the active site of cruzain was carried out using the software AutoDock Vina 1.1.2 [23]. The crystallographic structure of cruzain in complex with vinyl sulfone derived inhibitor (WRR-483) was retrieved from the Protein Data Bank (PDB ID: 3LXS). Then, the structure of the cruzain was prepared using the software UCSF Chimera [24], which removes all ligands and water molecules of the receptor structure, also repairs missing side chains and adds polar hydrogens. On the other hand, the co-crystallized ligand WRR-483 and the BAH and BAH-N series were prepared using UCSF Chimera, this tool minimized the structures of each ligand and adds polar hydrogens to them. After, ligands and the receptor, both were converted to pdbqt format for run vina, using MGLTools 1.1.6 [25]. The docking search space had values of size $X = 60$, $Y = 60$, $Z = 60$ and was centered at $X = 52.15$, $Y = -3.633$ and $Z = 21.779$. The interactions between cruzain and the docked poses were calculated using Protein–Ligand Interaction Profiler (PLIP) [26].

RNA extraction from epimastigotes

BHI medium supplemented with 10% FBS and 1% penicillin–streptomycin 500 µg/mL was prepared and 90 µL of epimastigotes (1×10^6 cells/mL) and 10 µL of compound **9** and **12**, respectively, were added to a final concentration of 50 µg/mL to a 96-well plate. Aliquots were taken in triplicate at different times: 0, 2, 4, 6, 8, 12, 24 and 48 h, and the plate was kept in incubation at 28 °C for 48 h. Total RNA extraction was performed using the commercial kit SV Total RNA Isolation System (Promega®) according to the manufacturer's instructions. Total RNA quantification was performed on a Thermo Scientific® Nanodrop 2000.

Synthesis of cDNA from epimastigotes NINOA strain

Previously, 2 ng/µL of total RNA was incubated at 70 °C for 10 min, then centrifuged for 30 s and kept on ice. cDNA synthesis was performed according to Promega® commercial transcription protocol A3500. Reverse transcription reactions were prepared to contain 25 mM $MgCl_2$, 10X reverse transcription buffer, 10 mM dNTPs, 1 U/µL ribonuclease inhibitor, 25 U/µL reverse transcriptase, 0.5 µg/µL oligonucleotide $(dT)_{15}$ and adjusted to a final volume of 20 µL with nuclease-free water. Finally, the reactions were incubated in a SimpliAmp Thermal Cycler® at 42 °C for 15 min, then heated to 95 °C for 5 min and incubated at 5 °C for 5 min.

Analysis of the expression of the cruzain gene

The expression levels of the cruzain gene in the epimastigotes (NINOA strain) exposed to compounds **9** and **12**, respectively, at the concentration of 50 µg/mL (time 0, 2, 4, 6, 8, 12, 24 and 48 h) were compared with time zero in all cases. Primers for amplify cruzain gene and reaction conditions previously reported by Mejía-Jaramillo et al. [27] were used. The *gapdh* gene was used as a normalizing gene since its expression is constitutive and maintains similar levels of expression in the three forms of *T. cruzi* [28, 29]. Each reaction mixture contained 1 µL cDNA, 5 µL Green Supermix, 1 µL of each specific primer (GADPH-F: 5′-ACGGGC ATGTCTTTTCGTGT-3′ and GADPH-R: 5′-TGGAGCTGC GGTTGTCATT-3′) and the final volume was adjusted to 10 µL with sterile MiliQ water. The amplification was run on the CFX96 Real-Time System, BIO RAD® equipment. A standard deviation of ± 1 and a significance level of 95% ($p < 0.05$) was considered for relative quantification using the BIO RAD CFX Manager Version 3.1 software. The data was analyzed in GraphPad Prism 6 and the comparison of means by Tukey was made for those data that were significant ($p < 0.05$).

Results and discussion

Chemistry

Synthesis of the benzeneacylhydrazone (BAH series) derivatives (compounds from **1** to **7**) was carried out with high yields after the condensation of benzhydrazide with the appropriate aldehyde in ethanol using drops of hydrochloric acid as a catalyst. In the spectrum of the ^{1}H-NMR analysis,

the presence of a signal corresponding to the N=CH bond and a characteristic signal belonging to the N–H bond was observed, this was consistent for each derivative (^{1}H (400 MHz) and ^{13}C (101 MHz) NMR spectra were recorded with TMS as internal standard. Assignment of the NMR signals was made by HMQC and HMBC 2D methods). Also, all derivatives were structurally confirmed by IR, NMR, UPLC-MS *m/z*, and their melting point was determined. The compounds 1–7 previously have been reported and their characterization data were consistent with the previous reports [30–35].

***N′-[benzylidene]benzeneacylhydrazone* (1)** This compound was obtained in 47.63% from benzhydrazide and benzaldehyde. FT-IR (ν cm^{-1}): 3175 (w, N–H), 1639 (s, C=O), 1600 (s, C=N). ^{1}H NMR (400 MHz, DMSO-d_6) δ 7.38–7.49 (m, 3H, H-3″, H-4″), 7.51 (tt, J = 7.8, 1.3 Hz, 2H, H-3′), 7.59 (t, J = 7.3 Hz, 1H, H-4′), 7.73 (s, 2H, H-2″), 7.92 (d, J = 7.2 Hz, 2H, H-2′), 8.49 (s, 1H, H-4), 11.77 (s, 1H, NH). ^{13}C NMR (101 MHz, DMSO-d_6) δ 126.9 (C-2″), 127.5 (C-2′), 128.3 (C-3′), 128.7 (C-3″), 129.9 (C-4″), 131.5 (C-4′), 133.4 (C-1′), 134.3 (C-1″), 147.8 (C-4), 163.1 (C-1). *m/z* calculated: 224.09 Da, found: 225.15 $[M+H]^+$ Da; Retention Time: 0.820 min. Melting Point: 211 °C.

***N′-[(4-ethylphenyl)methylidene]benzeneacylhydrazone* (2)** This compound was obtained in 67.12% from benzhydrazide and 4-ethylbenzaldehyde. FT-IR (ν cm^{-1}): 3186 (w, N–H), 1643 (s, C=O), 1604 (s, C=N). ^{1}H NMR (400 MHz, DMSO-d_6) δ 1.20 (t, J = 7.6 Hz, 3H, H-6″), 2.64 (q, J = 7.9 Hz, 2H, H-5″), 7.29 (d, J = 7.9 Hz, 2H, H-3″), 7.51 (t, J = 7.3 Hz, 2H, H-3′), 7.54–7.59 (m, 1H, H-4′), 7.59–7.67 (m, 2H, H-2″), 7.87–7.98 (m, 2H, H-2′), 8.48 (s, 1H, H-4), 11.75 (s, 1H, NH). ^{13}C NMR (101 MHz, DMSO-d_6) δ 15.1 (C-6″), 28.07 (C-5″), 127.0 (C-2″), 127.5 (C-2′), 128.1 (C-3″), 128.3 (C-3′), 131.5 (C-4′), 131.8 (C-1″), 133.5 (C-1′), 146.0 (C-4″), 163.0 (C-1). *m/z* calculated: 252.31 Da, found: 253.15 $[M+H]^+$ Da; Retention time: 1.095 min. Melting point: 127 °C.

***N′-[(4-hydroxyphenyl)methylidene]benzeneacylhydrazone* (3)** This compound was obtained in 72.65% from benzhydrazide and 4-hydroxybenzaldehyde. FT-IR (ν cm^{-1}): 3184 (w, N–H), 1598 (s, C=O), 1547 (s, C=N). ^{1}H NMR (400 MHz, DMSO-d_6) δ 6.85 (d, J = 8.9 Hz, 2H, H-3″), 7.50 (t, J = 7.3 Hz, 2H, H-3′), 7.56 (d, J = 7.0 Hz, 2H, H-2″), 7.91 (d, J = 6.9 Hz, 2H, H-2′), 8.39 (s, 1H, H-4), 11.60 (s, 1H, NH). ^{13}C NMR (101 MHz, DMSO-d_6) δ 115.6 (C-3′) 127.4 (C-2′), 128.3 (C-3′), 128.7 (C-2″), 131.4 (C-1′), 133.6 (C-1″), 148.2 (C-4), 159.3 (C-4′), 162.8 (C-1). *m/z* calculated: 240.26 Da, found: 241.10 $[M+H]^+$ Da; Retention time: 0.810 min. Melting point: 228 °C.

***N′-[(4-methoxyphenyl)methylidene]benzeneacylhydrazone* (4)** This compound was obtained in 93.08% from benzhydrazide and 4-methoxybenzaldehyde. FT-IR (ν cm^{-1}): 3191 (w, N–H), 1639 (s, C=O), 1601 (s, C=N). ^{1}H NMR (400 MHz, DMSO-d_6) δ 3.81 (s, 3H, OCH_3), 7.02 (d, J = 8.6 Hz, 2H, H-2″), 7.51 (t, J = 7.3 Hz, 2H, H-3′), 7.58 (t, J = 7.2 Hz, 1H, H-4′), 7.67 (d, J = 7.4 Hz, 2H, H-3″), 7.90 (d, J = 7.2 Hz, 2H, H-2′), 8.41 (s, 1H, H-4), 11.63 (s, 1H, NH). ^{13}C NMR (101 MHz, DMSO-d_6) δ 55.2 (OCH_3), 114.3 (C-2″), 126.9 (C-1″), 127.4 (C-2′), 128.3 (C-3′), 128.5 (C-2″), 131.4 (C-4′), 133.6 (C-1′), 147.7 (C-4), 160.8 (C-4″), 162.9 (C-1). *m/z* calculated: 254.28 Da, found: 255.14 $[M+H]^+$ Da; Retention time: 0.911 min. Melting point: 143 °C.

***N′-[(4-fluorophenyl)methylidene]benzeneacylhydrazone* (5)** This compound was obtained in 91.59% from benzhydrazide and 4-fluorobenzaldehyde. FT-IR (ν cm^{-1}): 3058 (w, N–H), 1631 (s, C=O), 1600 (s, C=N). ^{1}H NMR (400 MHz, DMSO-d_6) δ 7.01 (t, J = 8.2 Hz, 2H, H-3″), 7.31–7.41 (m, 2H, H-3′), 7.43–7.50 (m, 1H, H-4′), 7.63–7.73 (m, 2H, H-2″), 7.87 (t, J = 7.2 Hz, 2H, H-2′), 8.36 (s, 1H, H-4), 11.49 (s, 1H, N*H*). ^{13}C NMR (101 MHz, DMSO-d_6) δ 115.0 (d, J = 21.8 Hz, C-3″), 127.2 (C-2′), 127.7 (C-3′), 128.8 (d, J = 8.3 Hz, C-2″), 129.9 (C-1″), 131.1 (C-4′), 133.2 (C-1′), 146.7 (C-4), 163.1 (d, J = 249.8 Hz, C-4″), 163.9 (C-1). *m/z* calculated: 242.25 Da, found: 243.12 $[M+H]^+$ Da; Retention time: 0.938 min. Melting point: 186 °C.

***N′-[(2-nitrophenyl)methylidene]benzeneacylhydrazone* (6)** This compound was obtained in 72.20% from benzhydrazide and 2-nitrobenzaldehyde. FT-IR (ν cm^{-1}): 3252 (w, N–H), 1673 (s, C=O), 1644 (s, C=N), 1522 (s, NO_2). ^{1}H NMR (400 MHz, DMSO-d_6) δ 7.51–7.57 (m, 2H, H-3′), 7.58–7.65 (m, 1H, H-4′), 7.66–7.71 (m, 1H, H-5″), 7.82 (t, J = 7.5 Hz, 1H, H-4″), 7.91–7.99 (m, 2H, H-2′), 8.05–8.10 (m, 1H, H-6″), 8.14 (s, 1H, H-3″), 8.92 (s, 1H, H-4), 12.20 (s, 1H, N*H*). ^{13}C NMR (101 MHz, DMSO-d_6) δ 124.4 (C-6″), 127.5 (C-2′), 127.7 (C-3″), 127.8 (C-1′), 128.3 (C-3′), 128.5 (C-1″), 130.5 (C-5″), 131.7 (C-4′), 133.5 (C-4″), 142.7 (C-4), 148.2 (C-2″), 165.8 (C-1). *m/z* calculated: 269.26 Da, found: 270.08 $[M+H]^+$ Da; Retention time: 0.940 min. Melting point: 202 °C.

***N′-[(4-nitrophenyl)methylidene]benzeneacylhydrazone* (7)** This compound was obtained in 80.70% from benzhydrazide and 4-nitrobenzaldehyde. FT-IR (ν cm^{-1}): 3182 (w, N–H), 1716 (s, C=O), 1644 (s, C=N), 1518 (s, NO_2). ^{1}H NMR (400 MHz, DMSO-d_6) δ 7.54 (t, J = 7.4 Hz, 2H, H-3′), 7.61 (t, J = 7.3 Hz, 1H, H-4′), 7.93 (d, J = 7.6 Hz, 2H, H-2′), 7.98 (d, J = 8.8 Hz, 2H, H-2″), 8.29 (d, J = 8.4 Hz, 2H, H-3″), 8.56 (s, 1H, H-4), 12.05 (s, 1H, N*H*). ^{13}C NMR (101 MHz, DMSO-d_6) δ 123.9 (C-3″), 127.6 (C-2′), 127.8 (C-2″), 128.3

(C-3′), 131.7 (C-4′), 133.1 (C-1′), 140.6 (C-1″), 145.1 (C-4), 147.8 (C-4″), 163.2 (C-1). *m/z* calculated: 269.26 Da, found: 270.05 $[M+H]^+$ Da; Retention time: 0.942 min. Melting point: 241 °C.

The *N*-propionyl-*N*′-benzeneacylhydrazone (BAH-N series) derivatives (compounds from **8** to **14**) were obtained with moderate yields, from the hydrazinolysis of propionyl chloride using compounds from **1** to **7** and triethylamine as a catalyst in dry dichloromethane and at 0 °C. In the spectrum of the ^{1}H NMR analysis, the absence of the signal for the N–H bond and the appearance of a new signal for the *N*-propionyl chain were observed. Additionally, all derivatives were confirmed structurally by IR spectroscopy, UPLC-MS (*m/z*) and their melting point were determined.

***N-propionyl-N′-[phenylmethylidene]benzeneacylhydrazone* (8)** This compound was obtained in 4.17% yield from compound **1** and propionyl chloride. FT-IR (ν cm^{-1}): 2938 (m, C–H), 1690 (s, C=O), 1670 (s, C=O), 1598 (s, C=N), 1234 (m, C–N). ^{1}H NMR (400 MHz, DMSO-d_6) δ 1.13 (t, J = 7.4 Hz, 3H, H-3‴), 2.91 (q, J = 7.4 Hz, 2H, H-2‴), 7.41–7.50 (m, 3H, H-3″ and H-4″), 7.50–7.57 (m, 2H, H-3′), 7.62–7.68 (m, 1H, H-4′), 7.76 (dd, J = 7.7, 1.8 Hz, 2H, H-2″), 7.80 (dd, J = 8.4, 1.3 Hz, 2H, H-2′), 8.29 (s, 1H, H-4). ^{13}C NMR (101 MHz, DMSO-d_6) δ 8.4 (C-3‴), 28.1 (C-2‴), 127.5 (C-2″), 128.6 (C-3′), 128.7 (C-3″), 129.2 (C-2′), 131.0 (C-4″), 133.3 (C-4′), 133.4 (C-1″), 133.7 (C-1′), 153.4 (C-4), 172.3 (C-1), 175.6 (C-1‴). *m/z* calculated: 280.32 Da, found: 281.10 $[M+H]^+$ Da; Retention time: 1.824 min. Melting point: 25–30 °C.

***N-propionyl-N′-[(4-ethylphenyl)methylidene]benzeneacylhydrazone* (9)** This compound was obtained in 8.47% yield from compound **2** and propionyl chloride. FT-IR (ν cm^{-1}): 2960 (m, C–H), 1693 (s, C=O), 1617 (s, C=O), 1598 (s, C=N), 1210 (m, C–N). ^{1}H NMR (400 MHz, DMSO-d_6) δ 1.11 (t, J = 7.4 Hz, 3H, H-3‴), 1.18 (t, J = 7.6 Hz, 3H, H-6″), 2.64 (q, J = 7.5 Hz, 2H, H-5″), 2.89 (q, J = 7.4 Hz, 2H, H-2‴), 7.30 (d, J = 8.2 Hz, 2H, H-2″), 7.48–7.56 (m, 2H, H-3′), 7.60–7.70 (m, 3H, H-4′ and H-3″), 7.78 (dd, J = 8.4, 1.3 Hz, 2H, H-2′), 8.26 (s, 1H, H-4). ^{13}C NMR (101 MHz, DMSO-d_6) δ 8.5 (C-3‴), 15.2 (C-6″), 28.1 (C-5″), 28.2 (C-2‴), 127.7 (C-2″), 128.2 (C-3″), 128.7 (C-3′), 129.2 (C-2′), 130.9 (C-1″), 133.3 (C-4′), 133.9 (C-1′), 147.4 (C-4″), 154.4 (C-4), 172.3 (C-1), 175.6 (C-1‴). *m/z* calculated: 308.15 Da, found: 309.13 $[M+H]^+$ Da; Retention time: 1.300 min. Melting point: 58 °C.

***N-propionyl-N′-[(4-hydroxyphenyl)methylidene]benzeneacylhydrazone* (10)** This compound was obtained in 60.06% yield from compound **3** and propionyl chloride. FT-IR (ν cm^{-1}): 2977 (m, C–H), 1747 (s, C=O), 1650 (s, C=O), 1541 (s, C=N), 1283 (m, C–N). ^{1}H NMR (400 MHz, DMSO-d_6) δ 1.15 (t, J = 7.5 Hz, 3H, H-3‴), 2.62 (q, J = 7.5 Hz, 2H, H-2‴), 7.23 (d, J = 8.3 Hz, 2H, H-2″), 7.53 (t, J = 7.3 Hz, 2H, H-3′), 7.56–7.62 (m, 1H, H-4′), 7.78 (d, J = 7.8 Hz, 2H, H-3″), 7.93 (d, J = 7.4 Hz, 2H, H-2′), 8.50 (s, 1H, H-4), 11.85 (s, 1H, O*H*). ^{13}C NMR (101 MHz, DMSO-d_6) δ 8.7 (C-3‴), 26.9 (C-2‴), 122.2 (C-3″), 127.5 (C-2′), 128.1 (C-2″), 128.4 (C-3′), 131.6 (C-1″), 131.9 (C-4′), 133.4 (C-1′), 146.9 (C-4), 151.7 (C-4″), 163.1 (C-1), 172.3 (C-1‴). *m/z* calculated: 296.32 Da, found: 297.06 $[M+H]^+$ Da; Retention time: 0.965 min. Melting point: 180 °C.

***N-propionyl-N′-[(4-methoxyphenyl)methylidene]benzeneacylhydrazone* (11)** This compound was obtained in 6.0% yield from compound **4** and propionyl chloride. FT-IR (ν cm^{-1}): 2924 (m, C–H), 1723 (s, C=O), 1618 (s, C=O), 1506 (s, C=N), 1247 (m, C–N). ^{1}H NMR (400 MHz, $CDCl_3$) δ 1.24 (t, J = 7.4 Hz, 3H, H-3‴), 2.93 (q, J = 7.4 Hz, 2H, H-2‴), 3.84 (s, 3H, OCH_3), 6.87–6.93 (m, 2H, H-3″), 7.39–7.47 (m, 2H, H-3′), 7.50–7.57 (m, 1H, H-4′), 7.59–7.64 (m, 2H, H-2″), 7.74–7.81 (m, 2H, H-2′), 8.17 (s, 1H, H-4). ^{13}C NMR (101 MHz, $CDCl_3$) δ 8.9 (C-3‴), 29.4 (C-2‴), 55.5 (O*C*H$_3$), 114.4 (C-3″), 126.5 (C-1″), 128.7 (C-3′), 129.6 (C-2′), 129.7 (C-2″), 133.2 (C-4′), 134.6 (C-1′), 153.9 (C-4), 162.3 (C-4″), 172.7 (C-1), 176.4 (C-1‴). *m/z* calculated: 310.13 Da, found: 311.05 $[M+H]^+$ Da; Retention time: 1.666 min. Melting point: 166 °C.

***N-propionyl-N′-[(4-fluorophenyl)methylidene]benzeneacylhydrazone* (12)** This compound was obtained in 88.58% yield from compound **5** and propionyl chloride. FT-IR (ν cm^{-1}): 2980 (m, C–H), 1707 (s, C=O), 1687 (s, C=O), 1601 (s, C=N), 1198 (m, C–N). ^{1}H NMR (400 MHz, DMSO-d_6) δ 1.11 (t, J = 7.4 Hz, 3H, C-3‴), 2.90 (q, J = 7.4 Hz, 2H, C-2‴), 7.30 (t, J = 8.9 Hz, 2H, H-3″), 7.49–7.56 (m, 2H, H-3′), 7.62–7.69 (m, 1H, H-4′), 7.76—7.98 (m, 4H, H-2″ and H-2′), 8.31 (s, 1H, H-4). ^{13}C NMR (101 MHz, DMSO-d_6) δ 8.47 (C-3‴), 28.11 (C-2‴), 115.93 (d, J = 22.1 Hz, C-3″), 128.72 (C-3′), 129.29 (C-2′), 129.9 (d, J = 8.8 Hz, C-2″) 130.1 (d, J = 3.0 Hz, C-1″), 133.46 (C-4′), 133.76 (C-1′), 152.30 (C-4), 163.68 (d, J = 249.2 Hz, C-4″), 172.37 (C-1), 175.75 (C-1‴). *m/z* calculated: 298.11 Da, found: 299.08 $[M+H]^+$ Da; Retention time: 2.171 min. Melting point: 82 °C.

***N-propionyl-N′-[(2-nitrophenyl)methylidene]benzeneacylhydrazone* (13)** This compound was obtained in 3.31% yield from compound **6** and propionyl chloride. FT-IR (ν cm^{-1}): 2976 (m, C–H), 1710 (s, C=O), 1691 (s, C=O), 1584 (s, C=N), 1507 (s, NO_2), 1243 (m, C–N). ^{1}H NMR (400 MHz, DMSO-d_6) δ 1.12 (t, J = 7.4 Hz, 3H, H-3‴), 2.91 (q, J = 7.4 Hz, 2H, H-2‴), 7.52–7.61 (m, 2H, H-3′), 7.67–7.75 (m, 2H, H-4″ and H-5″), 7.78–7.86 (m, 3H, H-2′

and H-4′), 8.04 (ddd, $J = 11.6$, 8.0, 1.3 Hz, 2H, H-3″ and H-6″), 8.48 (s, 1H, H-4). ^{13}C NMR (101 MHz, DMSO-d_6) δ 8.4 (C-3‴), 27.5 (C-2‴), 124.5 (C-3″ or C-6″), 127.8 (C-1″), 128.9 (C-3″ or C-6″), 129.0 (C-3′), 129.6 (C-2′), 131.3 (C-4″ or C-5″), 132.9 (C-1′), 133.6 (C-4′), 134.2 (C-4″ or C-5″), 145.8 (C-4), 172.6 (C-1), 176.0 (C-1‴). *m/z* calculated: 325.10 Da, found: 326.03 $[M+H]^+$ Da; Retention time: 1.875 min.

***N-propionyl-N′-[(4-nitrophenyl)methylidene]benzeneacylhydrazone* (14)** This compound was obtained in 6.91% yield from compound **7** and propionyl chloride. FT-IR (ν cm^{-1}): 2976 (m, C–H), 1710 (s, C=O), 1692 (s, C=O), 1585 (s, C=N), 1506 (s, NO_2), 1245 (m, C–N). ^{1}H NMR (400 MHz, DMSO-d_6) δ 1.13 (t, $J = 7.4$ Hz, 3H, H-3‴), 2.98 (q, $J = 7.4$ Hz, 2H, H-2‴), 7.51–7.61 (m, 2H, H-3′), 7.71 (tt, $J = 7.0$, 1.3 Hz, 1H, H-4′), 7.85 (dd, $J = 8.4$, 1.2 Hz, 2H, H-2′), 7.98–8.05 (m, 2H, H-3″), 8.23–8.33 (m, 2H, H-2″), 8.38 (s, 1H, H-4). ^{13}C NMR (101 MHz, DMSO-d_6) δ 8.3 (C-3‴), 27.6 (C-2‴), 123.9 (C-2″), 128.4 (C-3″), 129.0 (C-3′), 129.6 (C-2′), 133.1 (C-1′), 134.1 (C-4′), 139.7 (C-1″), 147.5 (C-4), 148.4 (C-4″), 172.7 (C-1), 176.2 (C-1‴). *m/z* calculated: 325.10 Da, found: 326.05 $[M+H]^+$ Da; Retention time: 1.865 min. Melting point: 101 °C.

Trypanocidal activity

The anti-*T. cruzi* activity of the BAH and BAH-N series (compounds from **1** to **14**) were evaluated against epimastigotes and trypomastigotes of the NINOA strain (Table 1). The IC_{50} was determined in those compounds that presented the highest percentage of mortality in epimastigotes. While for the most active compounds against trypomastigotes, the LC_{50} was calculated.

Epimastigotes

Compounds **1** and **2** of the BAH series showed low activity against *T. cruzi* epimastigotes, 10.4 and 10.8% mortality, respectively. However, compound **3** substituted with a –OH group at *para*-position on the phenyl ring, enhanced biological activity. This effect may be because the hydroxyl group is

Table 1 In vitro trypanocidal activity of benzeneacylhydrazone and *N*-propionyl-*N′*-benzeneacylhydrazone derivatives against *T. cruzi* NINOA strain

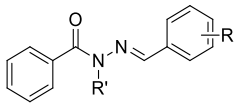

Compound	R	R′	% Mortality at 50 µg/mL	Epimastigotes IC_{50} (µM)[b]	% Mortality at 50 µg/mL	Trypomastigotes LC_{50} (µM)[b]
1	H	H	10.4	ND	31.2	ND
2	*p*-CH_2–CH_3	H	10.8	ND	40.1	ND
3	*p*-OH	H	24.5	ND	29.0	ND
4	*p*-OCH_3	H	5.2	ND	28.7	ND
5	*p*-Fluorine	H	0	ND	68.3	**202.68***
6	*o*-NO_2	H	0	ND	33.0	ND
7	*p*-NO_2	H	0	ND	46.2	**455.09***
8	H	–CO–CH_2–CH_3	5.1	ND	50.0	**238.29***
9	*p*-CH_2–CH_3	–CO–CH_2–CH_3	61.4	**78.66***	25	ND
10	*p*-OH	–CO–CH_2–CH_3	16.3	ND	28.2	ND
11	*p*-OCH_3	–CO–CH_2–CH_3	0	ND	30.2	ND
12	*p*-Fluorine	–CO–CH_2–CH_3	41.6	**166.28***	40.7	**309.38***
13	*o*-NO_2	–CO–CH_2–CH_3	0	ND	38.9	ND
14	*p*-NO_2	–CO–CH_2–CH_3	29.9	ND	18.9	ND
Nifurtimox			84.8	0.24	52.1	182.01
Benznidazole			82.8	17.29	46.2	227.55

[a]ND: not determined

[b]The results are means of three experiments

[c]Bold values indicates significant results ($p < 0.05$)

highly reactive and participates in the formation of reactive oxygen species (ROS) [36]. Subsequently, the incorporation of a methoxy group in compound **4** at *para*-position was unfavorable. Finally, the compounds **5** (*para*-F phenyl), **6** (*ortho*-NO_2 phenyl) and **7** (*para*-NO_2 phenyl) were inactive against *T. cruzi* epimastigotes from the NINOA strain, due to solubility problems in the culture medium.

The *N*-acylation of compound **1** to obtain compound **8** (BAH-N series) caused a drastic loss of activity. Compounds **10** (*para*-hydroxy phenyl) and **11** (*para*-methoxy phenyl) also had a decrease in activity. However, the *N*-acylation of compound **2** to obtain **9** significantly enhances its biological activity. Additionally, the trypanocidal effect of compounds **12** and **14** (*para*-F and *para*-NO_2 phenyl, respectively) considerably increased after *N*-acylation. However, compound **13** (*ortho*-NO_2-phenyl) proved to be inactive, although the compound has a nitro group associated with trypanocidal activity by ROS generation.

Trypomastigotes

In general, the compounds of the BAH series had good activity against trypomastigotes of *T. cruzi* (NINOA strain); in particular, compound **5** showed a higher level of activity than the reference drugs (Table 1).

Compound **1** produced 31.25% lysis against trypomastigotes. Compound **2** substituted with an ethyl group at *para*-position on the phenyl ring slightly increased its activity. However, compounds **3** with a highly reactive group (*para*-hydroxyphenyl) and **4** with weak electron-donating (*para*-methoxyphenyl) were not very active. Compound **5** (*para*-fluorophenyl) had the highest level of activity against trypomastigotes, even higher than the reference drugs Nfx and Bzn. This can be attributed to the presence of a fluorine atom (electron-withdrawing group) at *para* position on the phenyl ring, which is similar to that reported by Pontes-Espíndola et al. [37] who mention that the steric effect exerted by the size of the atomic radius of the halogen atom is important for the activity of the compounds against trypomastigotes.

Unexpectedly, the BAH-N series (*N*-acylation) did not show a greater effect than that of the BAH series (except compound **8**, 50% mortality). In particular, compounds **9**, **12**, and **14** showed a loss of activity, compounds **10** and **11** remained with almost the same percentage of lysis, and compounds **8** and **13** had enhanced trypanocidal activity. Therefore, the structural modification did not improve trypanocidal activity against trypomastigotes of NINOA strain.

Molecular docking

The molecular docking analysis aimed to identify the most favorable binding pose and interaction profile of each compound on the active site of cruzain. Initially, a re-docking of the cruzain complex co-crystallized with WRR-483 (PDB ID: 3LXS) was performed and the root mean square deviation (RMSD) was calculated to validate the methodology. A free energy of binding (FEB) value of − 9.8 kcal/mol was obtained for the WRR-483 and an RMSD value equal to 0.4576 Å, which was considered acceptable to perform the molecular modeling of the fourteen derivatives of the BAH and BAH-N series.

Table 2 The pattern of interactions between BAH and BAH-N series derivatives on the cruzain active site

Compound	FEB (Kcal/mol)	Interaction type[a]		
		Hydrogen bond	Hydrophobic	π-stacking
1	− 6	Gln19, Gly20, Cys22	Trp184	Trp184
2	− 6.8	Gln19	Gln19, Asp161, Trp184,Thr185	Trp184
3	− 6.5	Gln19	Gln19	Trp184
4	− 6.6	Gln19	Gln19, Trp184	Trp184
5	− 6	Gln19, Gly20, Cys22	Trp184	Trp184
6	− 6.5	Asp18	Lys17, Phe28, Tyr91, Thr185	–
7	− 6.6	Gln19	Gln19, Trp184	Trp184
8	− 6.4	Gln19	Trp184	Trp184
9	− 6.8	Gln19	Trp184, Thr185	Trp184
10	− 6.3	Gln19	Ala141, His162, Trp184	Trp184
11	− 6.5	Gln19	Gln19, Trp184	Trp184
12	− 6.5	Gln19	Ala141, His162	Trp184
13	− 6.5	Gln19	Ala141, His162, Trp184	–
14	− 6.7	Gln19	Gln19, Trp184	Trp184
WRR-483	− 9.8	Gln19, Gly66, Asp161	His162	His162

[a]Interactions were obtained using the PLIP online server

In general, the BAH series (compounds **1**–**7**) contains an FEB value between − 6 and − 6.8 kcal/mol. While the BAH-N series (compounds **8**–**14**) submitted values between − 6.3 and − 6.8 kcal/mol. Table 2 describes the FEB values and the interaction profile for each compound.

Furthermore, a visual inspection of the mode of cruzain binding of the highest-scoring compounds in molecular docking was performed. Compound **2** (*para*-ethylphenyl) obtained the most favorable FEB value in the BAH series and had hydrophobic interaction with Gln19, Asp161, Trp184 and Trp185, respectively. In addition, the oxygen of a carbonyl group acted as a hydrogen acceptor by forming a hydrogen bond with the nitrogen from Gln19. Finally, a π-stacking interaction with the indole group of Trp184 was detected (Fig. 3a). On the other hand, compound **4** (*para*-methoxyphenyl) showed interactions with Gln19 and Trp184 residues (Fig. 3b). The nitrogen from Gln19 formed a hydrogen bond with the oxygen in the carbonyl group. Likewise, the nitrogen from Trp184's indole bonded with the oxygen from the carbonyl group by a hydrogen bond. Phenyl of the hydrazone moiety had a hydrophobic interaction with Trp184 and an interaction π-stacking.

Compound **7** (*para*-nitrophenyl) of the BAH series (− 6.6 kcal/mol) interacted with Gln19, His162 and Trp184 forming a hydrogen bridge, respectively, with the oxygen of the carbonyl. It also interacted hydrophobically with Gln19 and Trp184 as well as an interaction π-stacking. However, these compounds showed poor or null biological activity against epimastigotes; therefore, there is no correlation between the FEB value and trypanocidal activity.

In general, the compounds of the BAH series in the molecular docking showed no influence of the substituents on the phenyl ring to interact on the active site of cruzain. However, the addition of the *N*-propionyl chain favored the formation of new hydrogen bridges with residues from cruzain subsites.

The highest scoring compounds in the molecular docking were **9** and **14** with an FEB value of − 6.8 and − 6.7 kcal/mol, respectively, followed by compounds **11**, **12**, and **13** (− 6.5 kcal/mol, respectively). Visual inspection of the cruzain-compound **9** (Fig. 3c) showed that the benzene-acyl moiety was oriented opposite to the Cys25 residue; therefore, it only formed hydrophobic contacts with Trp184 and Thr185. The *N*-propionyl chain was arranged in subsite S1 forming hydrogen bridges with Gln19 and the indol nitrogen from the Trp184 residue. The putative pose that compound 14 adopted was in subsite S1′ interacting hydrophobically with Gln19 and Trp184. In addition, oxygen from the *N*-acyl chain favored interaction with Gln19 to form hydrogen bridges.

On the other hand, compound **11** adopted a conformation in subsite S1′ to interact with Gln19 and Trp184 through hydrogen bridges between the oxygen of the carbonyl of the *N*-propionyl chain. Compound **12** (Fig. 3d) presented a conformation in subsite S1′ similar to compound **11** but interacted hydrophobically with two new residues (Ala141 and His162). Again, the *N*-acyl chain oxygen functioned as a hydrogen acceptor forming bonds with Gln19. Finally, compound **13** was coupled on subsite S1′ interacting hydrophobically with Ala141, His162, and Trp184, and the oxygen of

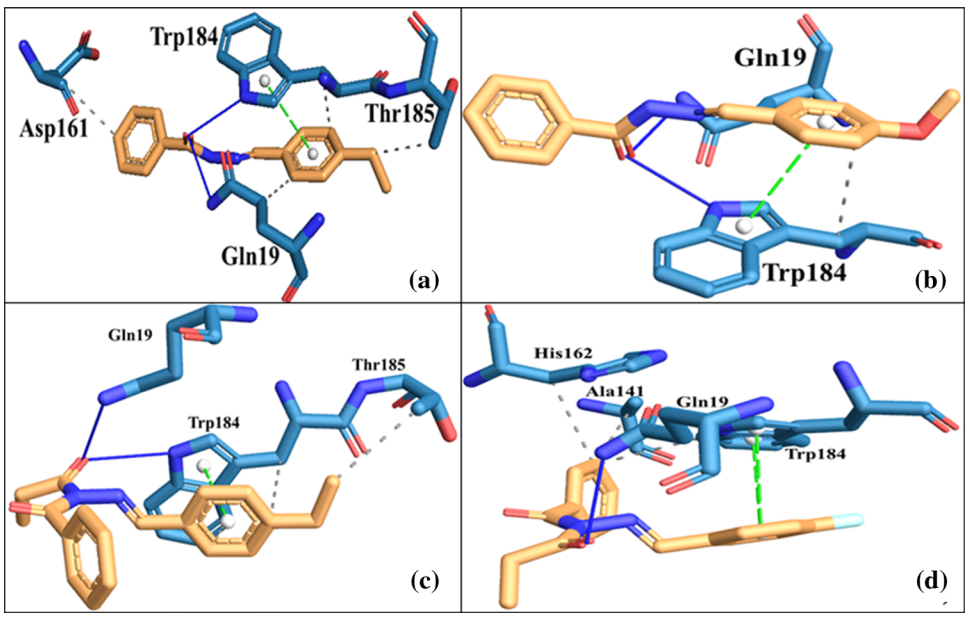

Fig. 3 The putative binding pose of BAH and BAH-N derivatives on the active site of the cruzain enzyme. **a** Compound **2**, **b** compound **4**, **c** compound **9**, **d** compound **12**. Hydrogen bonds are shown as blue lines and interaction hydrophobic as gray dashed lines. Green dashed lines represent π-stacking interactions

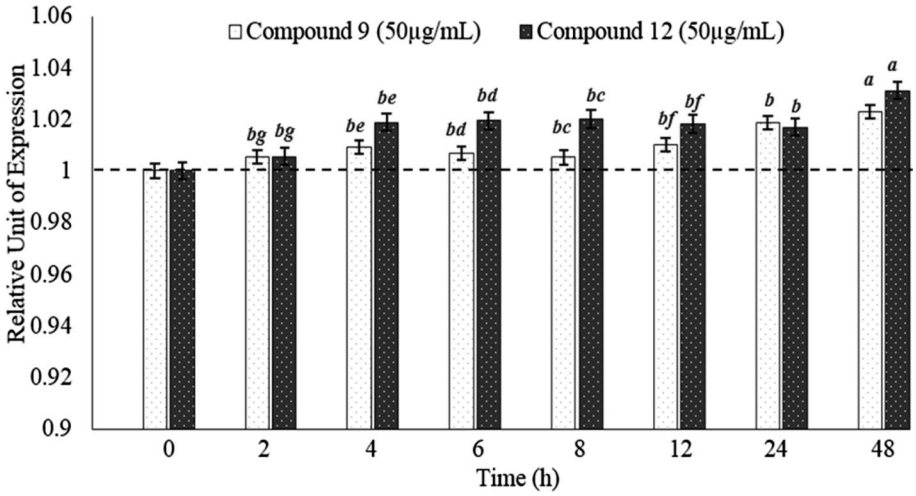

Fig. 4 Relative expression levels of the cruzain gene after treatment with compounds **9** and **12**, respectively. The dotted line represents the basal expression of the *gapdh* normalizer gene. ANOVA, $p < 0.05$. [a–g]Comparison of means by Tukey

the *N*-acyl chain interacted with Gln19 through hydrogen bridges.

Analysis of cruzain gene expression

An analysis to determine the expression levels of the cruzain gene in epimastigotes of *T. cruzi* after exposure to the derivatives **9** and **12** (50 µg/mL) was carried out to indirectly elucidate the possible mechanism of inhibition of the cruzain enzyme by these compounds. This according to Sajid et al. [38], who mentions that an increase in the expression levels of the cruzain gene, can occur in response to inhibition of the enzyme.

Relative quantification was used in the trial and the comparative method ΔCt was applied to establish the levels of expression of the cruzain gene with respect to the control. The determination of the expression of the constitutive gene *gapdh* allowed comparison with the expression of the cruzain gene after treatment with compound **9** and **12**, respectively. Thus, an increase of 0.01 relative units of expression could be observed from 2 h and the most pronounced increase was from 0.03 to 48 h for both treatments. This finding was significant ($p < 0.05$) when contrasted with time zero and with the *gapdh* gene (Fig. 4).

Conclusions

Seven derivatives of benzeneacylhydrazone (BAH) and seven of *N*-propionyl-*N*′-benzeneacylhydrazone (BAH-N) as potential trypanocidal agents and cruzain inhibitors were obtained. Compounds **9** and **12** showed the best activity against epimastigotes of the *T. cruzi* strain NINOA. On the other hand, compounds **5** and **8** presented an LC_{50} against trypomastigotes comparable to Bzn. The molecular docking analysis showed that all compounds interact strongly with Gln19 and Trp184 but not with Cys25 on the active site of cruzain. Finally, compounds **9** and **12** cause a significant increase in the expression of the cruzain gene at 48 h of exposure. These results display that the mechanism of action of compounds **9** and **12** could be by cruzain inhibition.

Acknowledgements This research was funded by Secretaria de Investigacion y Posgrado del Instituto Politecnico Nacional (SIP-20200491). Gildardo Rivera Sánchez and Benjamin Nogueda-Torres holds a scholarship from the "Comisión de Operación y Fomento de Actividades Académicas" (COFAA-IPN) and "Programa de Estímulos al Desempeño de los Investigadores" (EDI-IPN). José Carlos Espinoza-Hicks is thankful to the Consejo Nacional de Ciencia y Tecnología (CONACYT,Mexico) for a grant to purchase the NMR instrument (INFR-2014-01-226114).

Compliance with ethical standards

Conflict of interest None to declare.

References

1. Rassi A, Rassi A, Marin-Neto JA (2010) Chagas disease. Lancet 375:1388–1402
2. Coura JR, Borges-Pereira J (2010) Chagas disease: 100 years after its discovery. A systemic review. Acta Trop 115:5–13
3. Schmunis GA, Yadon ZE (2010) Chagas disease: a Latin American health problem becoming a world health problem. Acta Trop 115:14–21
4. Gascon J, Bern C, Pinazo MJ (2010) Chagas disease in Spain, the United States and other non-endemic countries. Acta Trop 115:22–27
5. Briceno L, Mosca W (2016) Quello che non si cerca difficilmente si trova: La malattia di Chagas. G Ital Cardiol 17:343–347
6. Center for Disease Control and Prevention. Parasites-American Trypanosomiasis (also known as Chagas Disease). https://www.cdc.gov/parasites/chagas/. Accessed 20 Dec 2017
7. World Health Organization. Sustaining the drive to overcome the global impact of neglected tropical diseases: second WHO

report on neglected diseases. https://www.who.int/news-room/fact-sheets/detail/chagas-disease-(american-trypanosomiasis). Accessed 27 April 2020
8. Wilkinson SR, Taylor MC, Horn D, Kelly JM, Cheeseman I (2008) A mechanism for cross-resistance to nifurtimox and benznidazole in trypanosomes. Proc Natl Acad Sci 105:5022–5027
9. Urbina JA (2010) Specific chemotherapy of Chagas disease: relevance, current limitations and new approaches. Acta Trop 115:55–68
10. Avila-Sorrosa A, Tapia-Alvarado JD, Nogueda-Torres B, Chacón-Vargas KF, Díaz-Cedillo F, Vargas-Díaz ME, Morales-Morales D (2019) Facile synthesis of a series of non-symmetric thioethers including a benzothiazole moiety and their use as effcient in vitro anti-trypanosoma cruzi agents. Molecules 24:3077
11. Avila-Sorrosa A, Bando-Vázquez AY, Alvarez-Alvarez V, Suarez-Contreras E, Nieto-Meneses R, Nogueda-Torres B, Vargas-Díaz ME, Díaz-Cedillo F, Reyes-Martínez R, Hernandez-Ortega S, Morales-Morales D (2020) Synthesis, characterization and preliminary in vitro trypanocidal activity of N-arylfluorinated hydroxylated-Schiff bases. J Mol Struct 1218:128520
12. Soeiro MNC, de Castro SL (2009) *Trypanosoma cruzi* targets for new chemotherapeutic approaches. Expert Opin Ther Targets 13:105–121
13. Doyle PS, Zhou YM, Hsieh I, Greenbaum DC, McKerrow JH, Engel JC (2011) The *Trypanosoma cruzi* protease cruzain mediates immune evasion. PLoS Pathog 7:1–11
14. Martinez-Mayorga K, Byler KG, Ramirez-Hernandez AI, Terrazas-Alvares DE (2015) Cruzain inhibitors: efforts made, current leads and a structural outlook of new hits. Drug Discov Today 20:890–898
15. Duarte CD, Barreiro EJ, Fraga CAM (2007) Privileged structures: a useful concept for the rational design of new lead drug candidates. Mini-Rev Med Chem 7:1108–1119
16. Welsch ME, Snyder SA, Stockwell BR (2010) Privileged scaffolds for library design and drug discovery. Curr Opin Chem Biol 14:347–361
17. Thota S, Rodríguez DA, de Pinheiro PSM, Lima LM, Fraga CAM, Barreiro EJ (2018) *N*-Acylhydrazones as drugs. Bioorg Med Chem Lett 28:2797–2806
18. Romeiro NC, Aguirre G, Hernández P, González M, Cerecetto H, Aldana I et al (2009) Synthesis, trypanocidal activity and docking studies of novel quinoxaline-*N*-acylhydrazones, designed as cruzain inhibitors candidates. Bioorg Med Chem 17:641–652
19. Massarico Serafim RA, Gonçalves JE, de Souza FP, de Melo Loureiro AP, Storpirtis S, Krogh R et al (2014) Design, synthesis and biological evaluation of hybrid bioisoster derivatives of *N*-acylhydrazone and furoxan groups with potential and selective anti-*Trypanosoma cruzi* activity. Eur J Med Chem 82:418–425
20. Elizondo-Jiménez S, Moreno-Herrera A, Reyes-Olivares R, Dorantes-González E, Nogueda-Torres B, Gamosa A, de Oliveira E et al (2017) Synthesis, biological evaluation and molecular docking of new benzenesulfonylhydrazone as potential anti-*Trypanosoma cruzi* agents. Med Chem 12:1–10
21. Norma Oficial Mexicana NOM-062-ZOO-1999 (1999) Especificaciones técnicas para la producción, cuidado y uso de los animales de laboratorio. In: Diario Oficial de la Federación
22. Brener Z (1962) Therapeutic activity and criterion of cure on mice experimentally infected with *Trypanosoma cruzi*. Rev Inst Med Trop Sao Paulo 4:389–439
23. Trott O, Olson AJ (2010) AutoDock Vina: improving the speed and accuracy of docking with a new scoring function, efficient optimization, and multithreading. J Comput Chem 31:455–461
24. Pettersen EF, Goddard TD, Huang CC, Couch GS, Greenblatt DM, Meng EC, Ferrin TE (2004) UCSF Chimera–a visualization system for exploratory research and analysis. J Comput Chem 25:1605–1612
25. Morris GM, Huey R, Lindstrom W, Sanner MF, Belew RK, Goodsell DS, Olson AJ (2009) Autodock4 and AutoDockTools4: automated docking with selective receptor flexibility. J Comput Chem 16:2785–2791
26. Salentin S, Schreiber S, Haupt VJ, Adasme MF, Schroeder M (2015) PLIP: fully automated protein-ligand interaction profiler. Nucleic Acids Res 43:W443–W447
27. Mejía-Jaramillo AM, Fernández GJ, Palacio L, Triana-Chávez O (2011) Gene expression study using real-time PCR identifies an NTR gene as a major marker of resistance to benznidazole in *Trypanosoma cruzi*. Parasites Vectors 4:169
28. Araújo PR, Burle-Caldas GA, Silva-Pereira RA, Bartholomeu DC, daRocha WD, Teixeira SMR (2011) Development of a dual reporter system to identify regulatory cis-acting elements in untranslated regions of *Trypanosoma cruzi* mRNAs. Parasitol Int 60:161–169
29. Tavernelli LE, Motta MCM, Silva Gonçalves C, Santos da Silva M, Elias MC, Alonso VL et al (2019) Overexpression of *Trypanosoma cruzi* High Mobility Group B protein (TcHMGB) alters the nuclear structure, impairs cytokinesis and reduces the parasite infectivity. Sci Rep 9:1–16
30. Zhang L, Zheng XF, Linn G, Zhao K (2007) Synthesis of 1,3-Disubstituted *N*-Amino-1,2,3,4-tetrahydroisoquinolines. Synlett 3:0374–0380
31. Ok DJ, Yoon KS (2009) Cinchona-alkaloid-based organic catalyst and a process of preparing chiral arylamine by using the same. National Center for Biotechnology Information. PubChem Patent Summary for KR-20100128182-A. https://pubchem.ncbi.nlm.nih.gov/patent/KR-20100128182-A. Accessed 9 Oct 2020
32. Tian Z, Qingchun Z, Qi H (2019) The preparation method of parahydroxyben-zaldehyde benzoyl hydrazone. National Center for Biotechnology Information. PubChem Compound Summary for CID 136470051, 4-Hydroxybenzaldehyde benzoyl hydrazone. https://pubchem.ncbi.nlm.nih.gov/compound/4-Hydroxybenzaldehyde-benzoyl-hydrazone. Accessed 9 Oct 2020
33. Masahiro H, Tomohiro K, Akihiko M, Kenichi S, Shigeki K, Yoshihisa T (2005) Rubber and tires composition. National Center for Biotechnology Information. PubChem Compound Summary for CID 5539485, *N*-[(Z)-(4-Methoxyphenyl) methylideneamino] benzamide. https://pubchem.ncbi.nlm.nih.gov/compound/5539485. Accessed 9 Oct 2020
34. Luhua L, Ying L, Qian W, Pei L (2016) D-3-phosphoglycerate dehydrogenase allosteric inhibitor and use thereof. National Center for Biotechnology Information. PubChem Compound Summary for CID 5397591, *N*-[(Z)-(4-Fluorophenyl)methylideneamino]benzamide. https://pubchem.ncbi.nlm.nih.gov/compound/5397591. Accessed 9 Oct 2020
35. Ibrahim AS, Ismail W, Mohammed A A, Iqbal CM, Atia-Tul W, Saima R (2013) Heterocyclic schiff's bases as novel and new anti-glycation agents. National Center for Biotechnology Information. PubChem Compound Summary for CID 5397599, *N*-[(Z)-(2-Nitrophenyl)methylideneamino]benzamide. https://pubchem.ncbi.nlm.nih.gov/compound/5397599. Accessed 9 Oct 2020
36. Machado-Silva A, Gonçalves Cerqueira P, Grazielle-Silva V, Ramos Gadelha F, de Figueiredo PE, Ribeiro Teixeira SM et al (2016) How *Trypanosoma cruzi* deals with oxidative stress: antioxidant defence and DNA repair pathways. Mutation Res Rev Mutation Res 767:8–22
37. Pontes Espíndola JW, de Oliveira Cardoso MV, de Oliveira Filho GB, Oliveira Silva DA, Magalhaes Moreira DR, Bastos TM et al (2015) Synthesis and structure activity relationship study of a new series of antiparasitic aryloxyl thiosemicarbazones inhibiting *Trypanosoma cruzi* cruzain. Eur J Med Chem 101:818–835
38. Sajid M, Robertson SA, Brinen LS, McKerrow JH (2011) Cruzain: the path from target validation to the clinic. Adv Exp Med Biol 712:100–115

Affiliations

Timoteo Delgado-Maldonado[1] · Benjamín Nogueda-Torres[2] · José C. Espinoza-Hicks[3] · Lenci K. Vázquez-Jiménez[1] · Alma D. Paz-González[1] · Alfredo Juárez-Saldívar[1] · Gildardo Rivera[1]

✉ Gildardo Rivera
gildardors@hotmail.com

[1] Laboratorio de Biotecnología Farmacéutica, Centro de Biotecnología Genómica, Instituto Politécnico Nacional, 88710 Reynosa, Mexico

[2] Departamento de Parasitología, Escuela Nacional de Ciencias Biológicas, Instituto Politécnico Nacional, 11340 Ciudad de México, Mexico

[3] Laboratorio de Química II, Departamento de Química Orgánica, Facultad de Ciencias Químicas, Universidad Autónoma de Chihuahua, Circuito Universitario, Campus Universitario, Apartado Postal 669, Chihuahua, Chih., Mexico